

11

Shear-Force-Controlled Scanning Ion Conductance Microscopy

Tilman E. Schäffer, Boris Anczykowski, Matthias Böcker,
and Harald Fuchs

11.1 Overview

In multicellular organisms structures such as endothelial or epithelial cell layers form the interface between different fluid compartments, and play an important role for inter- and transcellular processes [1, 2]. Gaining insight into the complex barrier-crossing transport mechanisms is a common interest of cell biology, medicine, and pharmacology, as malfunctioning of these barriers leads to pathological implications. In particular, knowledge about the permeability of barriers for substances such as drugs is highly relevant.

Hence, special electrochemical and microscopic methods are required to study the ion-permeability of barrier-forming cell structures. For example, experimental techniques such as the measurement of transepithelial electrical resistances (TER) provide valuable information about the barrier properties of cell layers [3–5]. In addition to such integrating measurements of the total cell layer impedance, there is a need for complementary microscopic methods which can provide additional information concerning topography and local ion conductance, as well as mechanical, optical, electrical or chemical properties, with spatial resolution down to the nanometer level. Today, these requirements are met by the variety of scanning probe microscopes currently available.

The first scanning tunneling microscope (STM) was constructed by Binnig, Rohrer and coworkers [6] in 1981, and these authors were awarded the Nobel Prize in 1986 for their achievement. This in turn triggered the development of a large family of new microscopes – the so-called scanning probe microscopes (SPM) – all of which are based on a small, locally confined probe that is sensitive to various physical quantities. The most prominent members of the group are the scanning near-field optical microscope (SNOM) [7] and the atomic force microscope (AFM) [8]. One of the main applications of the AFM is to create high-resolution topographic images of surfaces in different environmental conditions (including aqueous buffer solution), which makes it well suited to biological

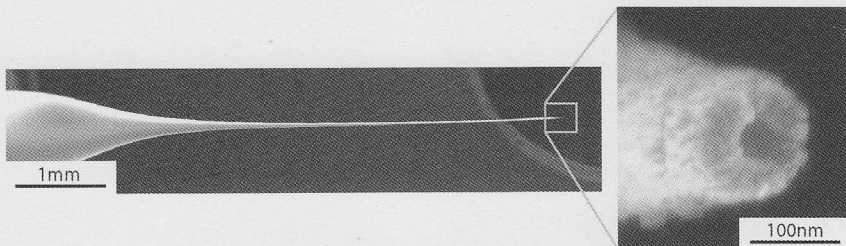


Fig. 11.1 Scanning electron microscopy (SEM) images of a nanopipette. Left: The tapered end of the nanopipette is several millimeters in length. Right: The inner opening diameter at the tip of the nanopipette is typically 30–100 nm. To improve SEM imaging, the nanopipette was sputter-coated with a thin layer of platinum.

applications [9]. Several related SPMs have been developed to date, including the magnetic force microscope (MFM) [10, 11], the electric force microscope [12], and the scanning electrochemical microscope (SECM) [13].

A scanning ion conductance microscope (SICM), which was invented by Hansma et al. in 1989 [14, 15], uses a local probe that is sensitive to ion conductance in an electrolyte solution. Drawn-out glass capillaries (“nanopipettes”), similar to those used in intracellular recording and patch-clamp experiments [16, 17], are well suited for this purpose. A nanopipette puller based on a heated coil or an infrared laser beam locally heats up a glass (e.g., borosilicate) capillary with an initial outer diameter of 1–2 mm that is subsequently drawn apart by force. This results in thin nanopipettes a few millimeters in length (Figure 11.1, left) that have sharp tips with typical opening diameters on the order of 30 to 100 nm (Figure 11.1, right). Opening diameters down to 13 nm were achieved when using quartz capillaries [18]. The use of microfabricated probes has also been reported [19].

The SICM scans a nanopipette over the surface of a sample that is immersed in electrolyte (Figure 11.2a). Two electrodes are placed in the electrolyte: one inside the thick end of the electrolyte-filled nanopipette (the “pipette electrode”), and one outside the nanopipette in the bath over or under the sample (the “bath electrode”). By applying a voltage between both electrodes and recording the ion current through the nanopipette, locally resolved images of ion conductance over the sample surface can be generated. Despite the many possible applications of such a microscope, the SICM is one of the least-developed scanning probe microscopy techniques to date. Only a few set-ups have been described in the literature [14, 15, 20–26].

There is a strong dependence of the measured current on the tip-sample distance (the “current squeezing effect”). The tip-sample distance can therefore be kept constant during scanning by using the current as an input to a feedback loop, thereby generating images of the sample topography. This works particularly well for nonporous samples where the bath electrode is positioned on the same side of the sample as the nanopipette. The pipette and sample do not

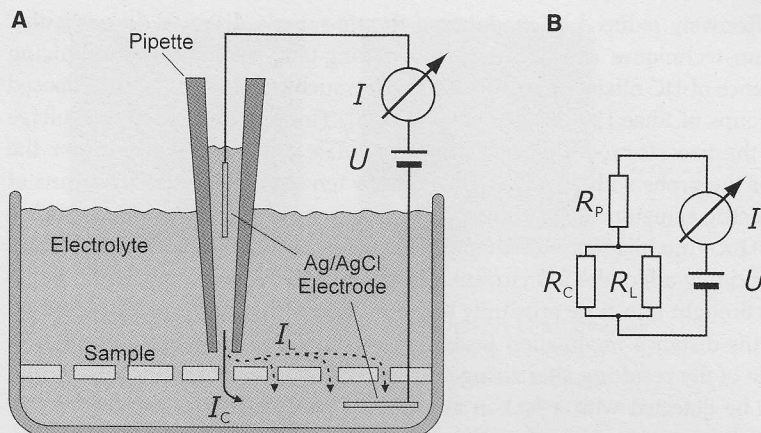


Fig. 11.2 (a) Schematic of the current measurement set-up. When a voltage U is applied between the two electrodes, an ion current flows through the opening of the nanopipette tip. Two alternate paths of the current through the sample are possible: either through a locally defined channel directly below the nanopipette tip (I_C), or through remote pores. As the second path is possible only when current “leaks” through the gap between nanopipette and sample, this current is called leakage current (I_L). The

closer the nanopipette tip is to the sample, the more this leakage current is restricted (“squeezed”) by the gap. (b) Equivalent circuit. The nanopipette resistance R_P is in series with a parallel configuration of the channel resistance R_C and the leakage resistance R_L . Usually, I_C is the quantity of interest. Therefore, the nanopipette resistance R_P should be as small as possible, and the leakage resistance R_L should be as large as possible, requiring the gap between nanopipette and sample to be small.

come into mechanical contact with each other, and soft and delicate samples can be imaged by using this “non-contact” configuration. Korchev et al., for example, imaged the topography of living cells with SICM [23] in order to monitor dynamic changes in cell volume at a resolution of $2.5 \times 10^{-20} \text{ l}$ [27] and to localize single active ion channels on the cell surface [28].

Advanced techniques and a number of different approaches have been conceived for overcoming some limitations and inherent problems of the original SICM concept. One possible option is to employ some type of point-spectroscopy technique, as it is known from other scanning probe methods such as atomic force microscopy [29]. Here, the probe is approached to and then retracted from the sample surface by typically several micrometers for each data point of the scanning area [30–32]. Although the risk of the probe laterally colliding with a protrusion on the surface or it becoming trapped in a depression is reduced, this is achieved at the price of very low scanning speed. Unwanted effects caused by slowly changing direct current (DC) potentials at the electrodes can be reduced for instance by applying either short voltage or current pulses instead of applying a constant voltage between the nanopipette and bath electrodes [31, 32].

Furthermore, modulation techniques have proved to be effective. These share the common idea that the risk of hitting a surface feature during lateral scanning

can be effectively reduced by modulating the tip-sample distance. In particular, modulation techniques can help to improve long-term stability by minimizing the influence of DC offsets and drift effects. One such method has been proposed by the groups of Shao [26, 33] and Korchev [25]. These authors keep the voltage between the two electrodes constant, but modulate the z-position of either the sample or the probe with an amplitude of a few tens of nanometers by means of a piezoelectric actuator. If the probe is far away from the sample surface, such a small distance modulation with a typical frequency of a few hundred Hertz does not significantly affect the ion current. However, if the tapered end of the nanopipette is brought into close proximity to the surface so that the “squeezing effect” sets in, this distance modulation leads to a modulation of the ion current. The amplitude of the resulting alternating current (AC) component in the ion current can then be detected with a lock-in amplifier. The latter allows the recovery of noisy, low-level ion current signals by using the voltage signal which modulates the tip-sample distance as a reference signal. The detected amplitude of the modulated ion current is then used as feedback signal to control the average tip-sample distance – that is, the feedback system tries to maintain a constant amplitude of the ion current while scanning the surface. This method of distance control has advantages over the conventional DC current-based approach because it makes the measurement less sensitive to changes in ionic strength or other DC drift effects.

Such advanced modulation techniques allow gentle scanning of delicate biological surfaces such as living cells. The improved performance of a distance-modulated SICM allows well-resolved images to be obtained of fine surface structures such as microvilli [34] or membrane proteins [18] on living cells. As the introduction of the distance-modulation technique reduces the risk of uncontrolled contact between the probe and sample, and also improves long-term stability, it becomes possible to continuously image specific surface areas for several hours and thereby to study dynamic processes [35, 36]. Gorelik et al., for example, studied the mechanism by which aldosterone activates sodium reabsorption via the epithelial sodium channel, and proposed a new hypothesis that is based on the effect of cell contraction (Figure 11.3) on the interaction of the channel with the F-actin cytoskeleton [37].

So far, we have considered only distance-control methods that are based exclusively on the measurement of ion conductance. Although this works well for samples with a homogeneous distribution of ion conductance, in many cases it is of interest to study inhomogeneities in the local ion conductance, such as those arising due to the presence of channels through a thin porous membrane. In these cases, a mechanism which is independent of the ion conductance is required to keep the tip-sample distance constant. For this purpose, two different techniques have been developed to date: (i) SICM with complementary AFM control [21]; and (ii) SICM with complementary shear-force control [24].

The first technique uses a bent nanopipette that is coated with a reflective metal layer and is scanned over the sample surface. With such a configuration, the sample topography can be imaged using a standard AFM measurement set-up. The

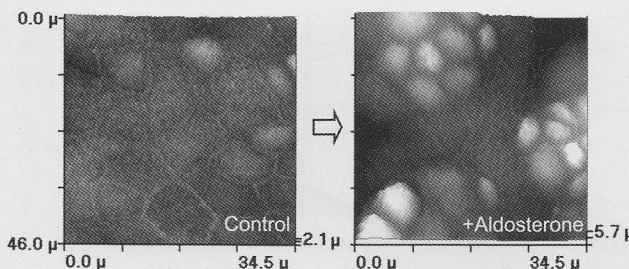


Fig. 11.3 Scanning ion conductance microscopy images of a monolayer of living A6 cells before (left) and 2 h after aldosterone stimulation (right). Prolonged cell morphology changes are observed, similar to changes induced by hypotonic stress. These changes do not occur in every cell, but rather in separate clusters of cells, and are likely the result of cell contraction. (Figure reprinted with permission from Ref. [37]; © 2005 National Academy of Sciences, USA.)

invention of the tapping mode in liquid [38, 39], which simplified the imaging of soft samples in solution, initiated the development of a novel microscope: Tapping-mode AFM combined with SICM [21]. In this design, the bent nanopipette [40, 41] is used both as a force sensor and an ion conductance probe. The bent nanopipette is vibrated perpendicularly to the sample surface with the help of a piezoelectric actuator. The excitation at the nanopipette's base leads to vibration amplitudes at the tip in the range of several nanometers to tens of nanometers. The measured vibration amplitude of the nanopipette serves as an input signal to a feedback loop that controls the nanopipette-sample distance, thereby generating the topography signal when scanning. Simultaneously, the ion current is recorded and used to generate a complementary image of the ion conductance. While such a microscope can also be operated in contact mode (using the DC deflection of the nanopipette), better resolution (both in topography and ion conductance) is generally obtained in tapping mode due to the absence of lateral imaging forces. The tapping mode-based SICM has been applied successfully in the field of biomineralization to investigate details of processes by which living organisms synthesize organic–inorganic composite materials [22].

In the case of shear-force-controlled SICM, a straight-tapered rather than a bent nanopipette is positioned perpendicularly to the sample surface and set into transverse vibrations (Figure 11.4). Arising mechanical shear-forces between the tip and sample provide an independent measure of sample topography. The combination of SICM with such a shear-force-based distance control allows the simultaneous and complementary imaging of sample topography and local ion conductance. Technological aspects as well as application examples of the shear-force based SICM will be discussed below.

The benefits of having two independent information channels are obvious: while the topographic data alone do not permit differentiation between a permeable ion-channel and a closed cavity in the cell layer, the ion current image pro-

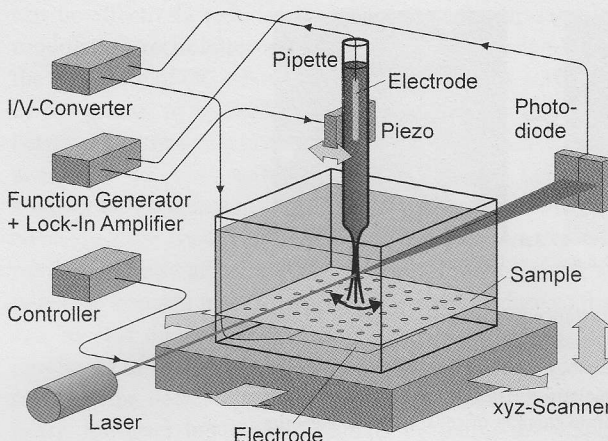


Fig. 11.4 Schematic of a shear-force-controlled scanning ion conductance microscope. A tapered nanopipette is brought into flexural vibrations by a piezoelectric actuator. The vibration amplitude is detected optically by focusing a laser beam onto the thin end of the nanopipette and directing the scattered beam onto a split photodiode. For low-noise amplitude determination, a lock-in amplifier is used whose reference channel is synchronized with the driving signal of the

piezoelectric actuator. When approaching the nanopipette to the sample surface, the vibration amplitude decreases due to arising shear forces. The vibration amplitude serves as input to a feedback loop, which keeps the nanopipette at constant distance to the sample surface during xy-scanning. The ion current through the nanopipette is recorded simultaneously, thereby revealing variations in the local ion conductance of the porous sample.

vides this important piece of information. Therefore, the combined set-up is an ideal tool for investigating local variations in the ion conductance of biological specimens. This is of special interest for research into the field of barrier-forming structures. Furthermore, the possibility of recognizing ionic transport channels in hard as well as soft samples opens perspectives for further applications in fields as diverse as biochemistry/pharmacology, corrosion research, quality control of coatings, or artificial membranes.

11.2

Methods

11.2.1

Shear-Force Detection

Shear-force detection is well known from SNOM set-ups, where the tip of a tapered optical fiber is scanned at a constant distance over a sample surface [42, 43]. In a shear-force configuration for SICM, a nanopipette is used instead of the fiber. The nanopipette is mounted perpendicularly to the sample surface (Figure 11.4), and a small piezoelectric actuator that is attached to the nanopipette pro-

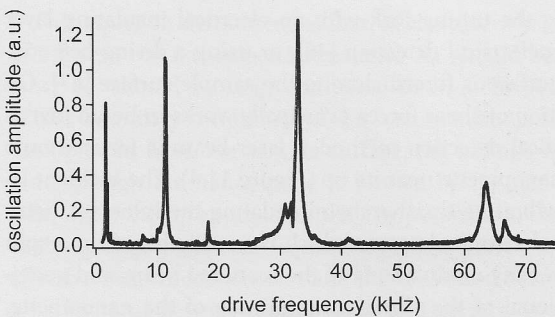


Fig. 11.5 Frequency spectrum of the oscillation of a driven nanopipette that is submerged into liquid electrolyte. Several resonances are typically present. For shear-force imaging, the piezoelectric actuator is driven at one of these resonances.

vides the driving signal that excites flexural mechanical vibrations in the drawn-out end of the nanopipette. The vibration amplitude depends heavily on the frequency of the driving signal, as the resonances in the system typically have a high quality factor (Figure 11.5). Several sharp peaks can be seen that indicate a strong oscillation of the nanopipette tip. When the oscillating nanopipette is approached to the surface, its vibration amplitude decreases sharply due to increasing shear forces at small tip-sample distances (Figure 11.6). The vibration amplitude is therefore well suited as a measure for the sample topography. The technical challenge is to find a method for detecting this vibration amplitude on the nanometer scale. To date, several methods have been established, including optical detection [42] and detection using a piezoelectric tuning fork sensor [44]. Piezoelectric detection methods face some principal problems when they are used for imaging in liquids, as electrical shorts may occur in the electrolyte medium. Solutions to

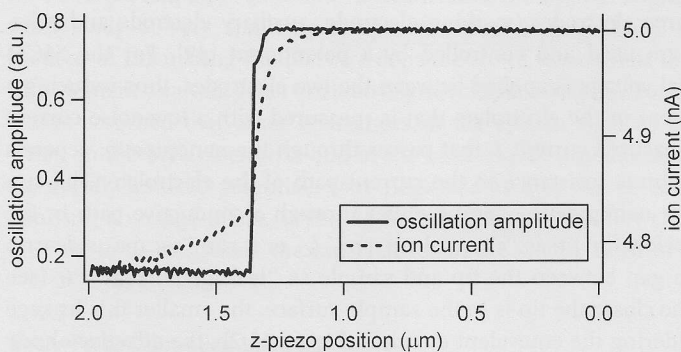


Fig. 11.6 Shear force oscillation amplitude and ion current while approaching a nanopipette to a sample surface. The shear force signal decreases sharply in close vicinity to the surface. The ion current also decreases (though less quickly), but already at larger tip-sample separations than the shear force signal.

this problem include coating the tuning fork with an electrical insulating layer [45], applying a custom piezoelectrical detection [46], or using a diving bell concept, where the water–air interface is forced close to the sample surface [47]. On the other hand, optical detection of shear forces principally works in liquid just as well as in air [48]. In the optical detection method, a laser beam is focused onto the vibrating section of the nanopipette near its tip (Figure 11.4). The incident laser beam is scattered by the vibrating tip, thereby modulating the intensity distribution of the beam. An optoelectronic detector, which is usually based on a split photodiode, detects these intensity modulations of the scattered beam and generates a signal that is proportional to the vibration amplitude of the nanopipette. There are two principal detection modes: detection in transmission and detection in reflection. The latter mode uses the nanopipette as a mirror, and requires the nanopipette to be coated with a reflective layer. It often produces a higher signal-to-noise ratio than the detection in transmission mode. The signal is then fed to a scan controller that keeps the tip-sample separation constant with the help of a feedback loop, thereby generating a topographic image of the sample surface while scanning.

11.2.2

Ion Current Measurement

Typical electrodes for the measurement of ion currents are standard silver/silver chloride (Ag/AgCl) electrodes that are also used as reference electrodes in potentiometry and voltammetry experiments. These are easily fabricated, for example by electrolytic deposition of a layer of silver chloride (AgCl) on a silver (Ag) wire. The Ag/AgCl electrode is described by a reversible redox reaction in which the chloride atoms in the solid silver chloride receive an electron and go into solution as chloride ions, leaving metallic silver. This reaction occurs close to the electrode surface (<1 nm distance). In SICM, two Ag/AgCl electrodes are used as the anode and cathode. This set-up is simpler to that used for voltammetric experiments, where three electrodes (working electrode, auxiliary electrode and reference electrode) are used and controlled by a potentiostat [49]. For the SICM set-up, an external voltage is applied between the two electrodes, thus inducing a Faradaic ion current in the electrolyte that is measured with a low-noise current amplifier. The measured current I , that passes through the nanopipette, depends on the effective ohmic resistance in the current path of the electrolyte. The current can leave the nanopipette opening either through a conductive path in the sample directly below the tip as “channel current” I_C , or it can “escape” sideways through the thin gap between the tip and sample as “leakage current”, I_L (see Figure 11.2b). The closer the tip is to the sample surface, the smaller this leakage current is. Considering the equivalent circuit in Figure 11.2b, the effective ohmic resistance in the current path, R_{eff} , can be expressed as:

$$R_{\text{eff}} = R_P + \frac{R_C R_L}{R_C + R_L}. \quad (1)$$

This equation demonstrates that, in the case when the channel resistance R_C is of interest, the nanopipette resistance R_P should be small and the leakage resistance R_L should be large compared to R_C . The resistances depend on the particular boundary conditions of the system such as the tip-sample distance: when the tip is far from the sample surface, the leakage resistance is zero and the current through the nanopipette is limited by the nanopipette resistance R_P . However, when the tip approaches the sample surface, the leakage resistance increases as the leakage current is “squeezed” by the narrowing gap [14, 50]. Therefore, the effective resistance increases and the measured current drops. In the ideal case of a perfect seal between nanopipette and surface at zero tip-sample distance, the current becomes zero at contact for a nonporous sample. Nitz et al. [24] constructed a simple analytical model for the distance-dependence of the measured current (in the absence of channels in the sample, i.e. $R_C \rightarrow \infty$). They obtained

$$I(z) \approx I_0 \left(1 + \frac{z_0}{z}\right)^{-1}, \quad (2)$$

where $I_0 = U/R_P$ is the measured current far away from the sample, U is the applied voltage, z the tip-sample separation, and z_0 is approximated by

$$z_0 = \frac{3r_0 r_i}{2L_P} \ln \frac{r_a}{r_i}. \quad (3)$$

The tapered nanopipette is assumed to be of conical shape with the inner diameter of the thick end r_0 , inner diameter of the thin end (at the nanopipette tip) r_i , outer diameter of the thin end r_a , and nanopipette length L_P (Figure 11.7, inset). When the tip approaches the surface, the measured current decreases to zero, with a characteristic length scale z_0 . For typical parameters ($r_0 = 0.3$ mm, $L_P = 5$ mm, $r_a = 50$ nm, $r_i = 30$ nm, $\rho = 1.09$ Ωm, $U = 100$ mV), we obtain $I_0 = 519$ pA and $z_0 = 0.60$ nm. In this model, the current begins to drop significantly only at very small tip-sample distances (Figure 11.7). A more detailed method of calculating the distance-dependence of the current that is based on finite element analysis gives qualitatively similar results [51]. For these derivations, it was assumed that other resistances in the system such as resistances in the wires, in the bulk electrolyte and in the solid–liquid junctions, are small. Electrochemically induced potentials were neglected as they can be compensated for by applying a voltage offset. It should be noted that, when fast changes of the current are to be measured, the capacitances in the system need to be considered.

11.2.3

Shear-Force-Controlled Imaging

In order to acquire images of sample conductance that are independent of topography, the nanopipette tip must be held at a constant position over the sample surface. The shear-force distance control serves this purpose, allowing the simul-

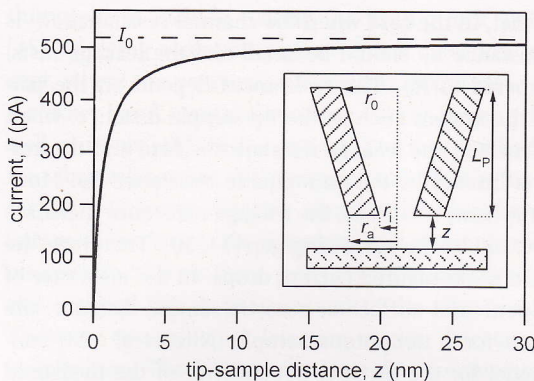


Fig. 11.7 Calculated current versus distance curve, based on a simple analytical model [Eq. (2) and inset]. The parameters used for calculating the curve were $r_0 = 0.3$ mm, $r_t = 30$ nm, $r_a = 50$ nm, $L_p = 5$ mm, $\rho = 1.09 \Omega\text{m}$ and $U = 100$ mV. It is apparent that the current starts to drop only at tip-sample distances well below the nanopipette tip radius.

taneous recording of images of sample topography and ion current [24]. It might appear that the effective vertical spring constant of a vertically oriented nanopipette is relatively large, imposing a possible threat to soft samples. On the other hand, the non-contact nature of shear-force imaging allows the scanning of surfaces with small tip-sample interaction forces. Soft samples as delicate as cells in liquid could be imaged with a shear-force set-up (Figure 11.8), and the cells were well resolved. Furthermore, shear-force-controlled SICM was used to provide further insight into transport mechanisms of cellular membranes. One example is the investigation of the functionality of tight junctions between living cells (Figure 11.9). Features that might be indicative of cell-cell contacts were resolved in

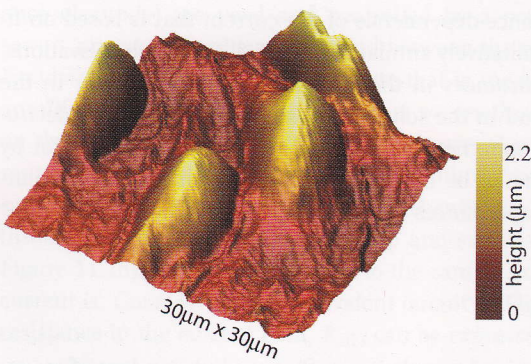


Fig. 11.8 Shear-force topography image of a monolayer of fixed MDCK-II cells on a glass support in buffer solution.

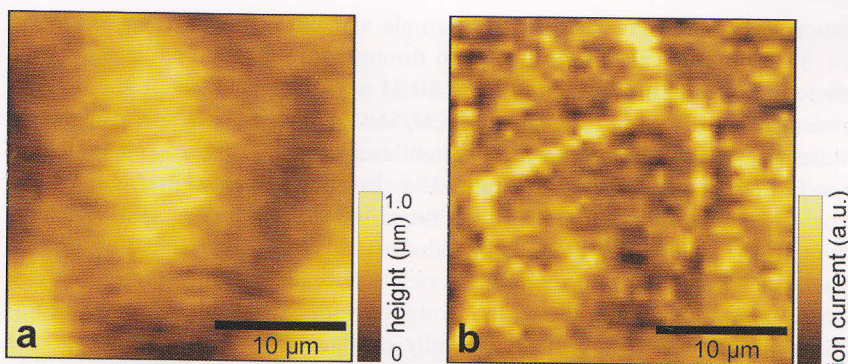


Fig. 11.9 Simultaneous (a) shear-force topography and (b) ion current images of a layer of live MDCK-II cells. Some, but not all, of the cell-cell contacts are visible in topography. The ion current image reveals lines of increased conductance that are independent of local surface topography. This finding suggests increased ion permeability through the tight junctions of the cell-cell contacts. (Sample provided by J. Seebach, experimental data by J. Kamp, University of Münster [51, 70].)

the ion current image as lines of increased conductance, even though the topography image did not reveal such features. This suggests that shear-force-controlled SICM is capable of measuring not only structural, but also functional, data on living cells.

11.3 Outlook

While the combined SICM and shear force microscope provides insight into cellular transport mechanisms and has a broad range of possible applications, further techniques which are based on similar components can be envisioned. The ability of the SICM to image biological samples *in vivo* with nanometer resolution makes it an interesting candidate for combination with other scanning microscopy techniques. For example, whilst adhering to the original SICM idea of using the ion current signal to maintain a constant distance between the scanning probe and the sample, complementary data, such as local optical data, can be recorded simultaneously. Combinations of SICM with scanning near-field optical microscopy (SNOM) or scanning confocal microscopy (SCM) are prominent examples.

The groups of Korchev and Shao modified the original SICM set-up in such a way that the end of the tapered nanopipette also serves as a near-field light source for SNOM [33, 52, 53]. This can be achieved by coupling laser light into the nanopipette via an optical fiber. Coating the outside of the nanopipette with a reflective metal layer helps to confine the laser light to the aperture – that is, the tapered

nanopipette's end. Provided that the sample and the substrate are transparent, the SNOM signal can then be collected through an objective and detected by a photomultiplier located underneath the SICM head. Living cells were successfully investigated with such a combined SICM/SNOM set-up. An alternative way to utilize the SICM probe as a confined light source for SNOM was suggested by Bruckbauer et al. [54, 55]. This method is based on fluorescence as it occurs when a calcium indicator, with which the nanopipette is filled, binds with calcium in the sample solution and is illuminated with a laser. The mixing zone where the fluorescent complex forms serves as a localized light source.

SICM has also been successfully combined with SCM [56]. The set-up comprises an inverted light microscope fully configured for SCM, on which the SICM head is placed. During lateral scanning the vertical position of the sample is controlled by a standard SICM, that is, by an ion-current-based feedback loop. As a consequence, the optical confocal volume, which is located just below the end of the nanopipette, follows the topography of the sample. This allows capturing of fluorescence images of a surface simultaneously with topographic data. Interaction of fluorescent nanoparticles (e.g., virus-like particles) with the surface of fixed or living cells can be studied in this way.

Another type of application is to employ the SICM to perform patch-clamp experiments at specific surface sites [34, 36]. In such experiments, the SICM is first used to scan the sample surface, and the spatially resolved images of the surface topography allow the identification of regions or structures of interest. The scan unit is then used to position the tapered SICM probe over a user-selected spot. Finally, the probe is engaged to the sample surface to form a gigohm seal for subsequent patch-clamp recording. This combination of high-resolution SICM scanning and patch-clamping allows ion channel recordings to be obtained on selective surface spots with lateral position control in the range of a few tens of nanometers. Such high precision is beyond the reach of conventional positioning methods such as those using light microscopy. With the SICM it becomes possible to investigate the activity of single ion channels on nanometer-sized structures on native biological samples such as living cells. For instance, a tapered SICM nanopipette can be positioned deliberately on top of a single microvillus on an epithelial cell and used for subsequent patch-clamp recording. In this way, individual K⁺ channels could be identified on the basis of the reversal potential of current-voltage curves [34].

Nanopipettes not only serve as analytical probes but can also be used as powerful tools for the controlled delivery of reagents, and for material deposition. The material flux from a nanopipette to a substrate can either be driven by electric fields, capillary forces, hydrostatic pressure, or by ultrasonic excitation. Such types of nanolithography have been applied successfully to deposit metals [57–60] and chemicals [61, 62], as well as biological substances such as DNA, proteins, or other biomolecules [63–68]. Having the ability to deliver substances in a controlled manner through the nanopipette of a SICM opens the perspective to study the effects of local drug delivery on biological specimens, thereby providing a nanoscopic tool for the drug-induced manipulation of individual cells [69].

nanopipette's end. Provided that the sample and the substrate are transparent, the SNOM signal can then be collected through an objective and detected by a photomultiplier located underneath the SICM head. Living cells were successfully investigated with such a combined SICM/SNOM set-up. An alternative way to utilize the SICM probe as a confined light source for SNOM was suggested by Bruckbauer et al. [54, 55]. This method is based on fluorescence as it occurs when a calcium indicator, with which the nanopipette is filled, binds with calcium in the sample solution and is illuminated with a laser. The mixing zone where the fluorescent complex forms serves as a localized light source.

SICM has also been successfully combined with SCM [56]. The set-up comprises an inverted light microscope fully configured for SCM, on which the SICM head is placed. During lateral scanning the vertical position of the sample is controlled by a standard SICM, that is, by an ion-current-based feedback loop. As a consequence, the optical confocal volume, which is located just below the end of the nanopipette, follows the topography of the sample. This allows capturing of fluorescence images of a surface simultaneously with topographic data. Interaction of fluorescent nanoparticles (e.g., virus-like particles) with the surface of fixed or living cells can be studied in this way.

Another type of application is to employ the SICM to perform patch-clamp experiments at specific surface sites [34, 36]. In such experiments, the SICM is first used to scan the sample surface, and the spatially resolved images of the surface topography allow the identification of regions or structures of interest. The scan unit is then used to position the tapered SICM probe over a user-selected spot. Finally, the probe is engaged to the sample surface to form a gigaohm seal for subsequent patch-clamp recording. This combination of high-resolution SICM scanning and patch-clamping allows ion channel recordings to be obtained on selective surface spots with lateral position control in the range of a few tens of nanometers. Such high precision is beyond the reach of conventional positioning methods such as those using light microscopy. With the SICM it becomes possible to investigate the activity of single ion channels on nanometer-sized structures on native biological samples such as living cells. For instance, a tapered SICM nanopipette can be positioned deliberately on top of a single microvillus on an epithelial cell and used for subsequent patch-clamp recording. In this way, individual K^+ channels could be identified on the basis of the reversal potential of current-voltage curves [34].

Nanopipettes not only serve as analytical probes but can also be used as powerful tools for the controlled delivery of reagents, and for material deposition. The material flux from a nanopipette to a substrate can either be driven by electric fields, capillary forces, hydrostatic pressure, or by ultrasonic excitation. Such types of nanolithography have been applied successfully to deposit metals [57–60] and chemicals [61, 62], as well as biological substances such as DNA, proteins, or other biomolecules [63–68]. Having the ability to deliver substances in a controlled manner through the nanopipette of a SICM opens the perspective to study the effects of local drug delivery on biological specimens, thereby providing a nanoscopic tool for the drug-induced manipulation of individual cells [69].

- D., Korchev, Y. E. (2006) Imaging proteins in membranes of living cells by high-resolution scanning ion conductance microscopy. *Angew. Chem. Int. Ed.* **45**, 2212–2216.
- 19** Prater, C. B., Hansma, P. K. (1991) Improved scanning ion-conductance microscope using microfabricated probes. *Rev. Sci. Instrum.* **62**, 2634–2638.
- 20** Olin, H. (1994) Design of a scanning probe microscope. *Meas. Sci. Technol.* **5**, 976–984.
- 21** Proksch, R., Lal, R., Hansma, P. K., Morse, D., Stucky, G. (1996) Imaging the internal and external pore structure of membranes in fluid: tapping mode scanning ion conductance microscopy. *Biophys. J.* **71**, 2155–2157.
- 22** Schäffer, T. E., Ionescu-Zanetti, C., Proksch, R., Fritz, M., Walters, D. A., Almqvist, N., Zaremba, C. M., Belcher, A. M., Smith, B. L., Stucky, G. D., et al. (1997) Does abalone nacre form by heteroepitaxial nucleation or by growth through mineral bridges? *Chem. Mater.* **9**, 1731–1740.
- 23** Korchev, Y. E., Bashford, C. L., Milovanovic, M., Vodyanoy, I., Lab, M. J. (1997) Scanning ion conductance microscopy of living cells. *Biophys. J.* **73**, 653–658.
- 24** Nitz, H., Kamp, J., Fuchs, H., (1998) A combined scanning ion-conductance and shear-force microscope. *Probe Microsc.* **1**, 187–200.
- 25** Shevchuk, A. I., Gorelik, J., Harding, S. E., Lab, M. J., Klenerman, D., Korchev, Y. E., (2001) Simultaneous measurement of Ca^{2+} and cellular dynamics: combined scanning ion conductance and optical microscopy to study contracting cardiac myocytes. *Biophys. J.* **81**, 1759–1764.
- 26** Pastré, D., Iwamoto, H., Liu, J., Szabo, G., Shao, Z. (2001) Characterization of AC mode scanning ion-conductance microscopy. *Ultramicroscopy* **90**, 13–19.
- 27** Korchev, Y. E., Gorelik, J., Lab, M. J., Sviderskaya, E. V., Johnston, C. L., Coombes, C. R., Vodyanoy, I., Edwards, C. R. W. (2000) Cell volume measurement using scanning ion conductance microscopy. *Biophys. J.* **78**, 451–457.
- 28** Korchev, Y. E., Negulyaev, Y. A., Edwards, C. R. W., Vodyanoy, I., Lab, M. J. (2000) Functional localization of single active ion channels on the surface of a living cell. *Nat. Cell Biol.* **2**, 616–619.
- 29** Radmacher, M., Cleveland, J. P., Fritz, M., Hansma, H. G., Hansma, P. K. (1994) Mapping interaction forces with the atomic force microscope. *Biophys. J.* **66**, 2159–2165.
- 30** Gitter, A. H., Bertog, M., Schulzke, J.-D., Fromm, M. (1997) Measurement of paracellular epithelial conductivity by conductance scanning. *Eur. J. Physiol.* **434**, 830–840.
- 31** Mann, S. A., Hoffmann, G., Hengstenberg, A., Schuhmann, W., Dietzel, I. D. (2002) Pulse-mode scanning ion conductance microscopy: A method to investigate cultured hippocampal cells. *J. Neurosci. Methods* **116**, 113–117.
- 32** Happel, P., Hoffmann, G., Mann, S. A., Dietzel, I. D. (2003) Monitoring cell movements and volume changes with pulse-mode scanning ion conductance microscopy. *J. Microsc.* **212**, 144–151.
- 33** Mannelquist, A., Iwamoto, H., Szabo, G., Shao, Z. (2001) Near-field optical microscopy with a vibrating probe in aqueous solution. *Appl. Phys. Lett.* **78**, 2076–2078.
- 34** Gorelik, J., Yuchun, G., Spohr, H. A., Shevchuk, A. I., Lab, M. J., Harding, S. E., Edwards, C. R. W., Whitaker, M., Moss, G. W. J., Benton, D. C. H., et al. (2002) Ion channels in small cells and subcellular structures can be studied with a smart patch-clamp system. *Biophys. J.* **83**, 3296–3303.
- 35** Gorelik, J., Shevchuk, A. I., Frolenkov, G. I., Diakonov, I. A., Lab, M. J., Kros, C. J., Richardson, G. P., Vodyanoy, I., Edwards, C. R. W., Klenerman, D., et al. (2003) Dynamic assembly of surface structures in

- living cells. *Proc. Natl. Acad. Sci. USA* **100**, 5819–5822.
- 36** Gorelik, J., Zhang, A., Shevchuk, A., Frolenkov, G. I., Sanchez, D., Lab, M. J., Vodyanoy, I., Edwards, C. R. W., Klenerman, D., Korchev, Y. E. (2002) The use of scanning ion conductance microscopy to image A6 cells. *Mol. Cell. Endocrinol.* **217**, 101–108.
- 37** Gorelik, J., Zhang, Y., Sánchez, D., Shevchuk, A., Frolenkov, G., Lab, M., Klenerman, D., Edwards, C., Korchev, Y. (2005) Aldosterone acts via an ATP autocrine/paracrine system: The Edelman ATP hypothesis revisited. *Proc. Natl. Acad. Sci. USA* **102**, 15000–15005.
- 38** Hansma, P. K., Cleveland, J. P., Radmacher, M., Walters, D. A., Hillner, P. E., Bezanilla, M., Fritz, M., Vie, D., Hansma, H. G., Prater, C. B., et al. (1994) Tapping mode atomic force microscopy in liquids. *Appl. Phys. Lett.* **64**, 1738–1740.
- 39** Putman, C. A. J., Werf, K. O. V. d., Grooth, B. G. D., Hulst, N. F. V., Greve, J. (1994) Tapping mode atomic force microscopy in liquid. *Appl. Phys. Lett.* **64**, 2454–2456.
- 40** Shalom, S., Lieberman, K., Lewis, A., Cohen, S. R. (1992) A micropipette force probe suitable for near-field scanning optical microscopy. *Rev. Sci. Instrum.* **63**, 4061–4065.
- 41** Lewis, A., Taha, H., Strinkovski, A., Manevitch, A., Khatchatourians, A., Dekhter, R., Amman, E. (2003) Near-field optics: from subwavelength illumination to nanometric shadowing. *Nat. Biotechnol.* **21**, 1378–1386.
- 42** Betzig, E., Trautman, J. K., Harris, T. D., Weiner, J. S., Kostelak, R. L. (1991) Breaking the diffraction barrier: optical microscopy on a nanometric scale. *Science* **5000**, 1468–1470.
- 43** Toledo-Crow, R., Yang, P. C., Chen, Y., Vaez-Iravani, M. (1992) Near-field differential scanning optical microscope with atomic force regulation. *Appl. Phys. Lett.* **60**, 2957–2959.
- 44** Karrai, K., Grober, R. D. (1995) Piezoelectric tip-sample distance control for near field optical microscopes. *Appl. Phys. Lett.* **14**, 1842–1844.
- 45** Rensen, W. H. J., van Hulst, N. F., Kämmer, S. B. (2000) Imaging soft samples in liquid with tuning fork based shear force microscopy. *Appl. Phys. Lett.* **77**, 1557–1559.
- 46** Brunner, R., Hering, O., Marti, O., Hollricher, O. (1997) Piezoelectrical shear-force control on soft biological samples in aqueous solution. *Appl. Phys. Lett.* **71**, 3628–3630.
- 47** Koopman, M., de Bakker, B. I., Garcia-Parajo, M. F., van Hulst, N. F. (2003) Shear force imaging of soft samples in liquid using a diving bell concept. *Appl. Phys. Lett.* **83**, 5083–5085.
- 48** Lambelot, P., Pfeffer, M., Sayah, A., Marquis-Weible, F. (1998) Reduction of tip-sample interaction forces for scanning near-field optical microscopy in a liquid environment. *Ultramicroscopy* **71**, 117–121.
- 49** Bockris, J. O., Reddy, A. K. N. (2000) *Modern Electrochemistry: Electrodics in Chemistry, Engineering, Biology, and Environmental Science*. 2nd edn. Plenum Publishing Corporation, New York.
- 50** Bard, A. J., Denuault, G., Lee, C., Mandler, D., Wipf, D. O. (1990) Scanning electrochemical microscopy: a new technique for the characterization and modification of surfaces. *Acc. Chem. Res.* **23**, 357–363.
- 51** Schäffer, T. E., Anczykowski, B., Fuchs, H. (2006) Scanning ion conductance microscopy. In: Bhushan, B., Fuchs, H. (Eds.), *Applied Scanning Probe Methods*. Springer-Verlag, Berlin, Heidelberg, New York, Vol. 2, pp. 91–119.
- 52** Korchev, Y. E., Raval, M., Lab, M. J., Gorelik, J., Edwards, C. R. W., Rayment, T., Klenerman, D. (2000) Hybrid scanning ion conductance and scanning near-field optical microscopy for the study of living cells. *Biophys. J.* **78**, 2675–2679.
- 53** Mannelquist, A., Iwamoto, H., Szabo, G., Shao, Z. (2002) Near field optical microscopy in aqueous solution:

- implementation and characterization of a vibrating probe. *J. Microsc.* **205**, 53–60.
- 54** Bruckbauer, A., Ying, L., Rothery, A. M., Korchev, Y. E., Klenerman, D. (2002) Characterization of a novel light source for simultaneous optical and scanning ion conductance microscopy. *Anal. Chem.* **74**, 2612–2616.
- 55** Rothery, A. M., Gorelik, J., Bruckbauer, A., Yu, W., Korchev, Y. E., Klenerman, D. (2003) A novel light source for SICM–SNOM of living cells. *J. Microsc.* **209**, 94–101.
- 56** Gorelik, J., Shevchuk, A., Ramalho, M., Elliott, M., Lei, C., Higgins, C. F., Lab, M. J., Klenerman, D., Krauzewicz, N., Korchev, Y. (2002) Scanning surface confocal microscopy for simultaneous topographical and fluorescence imaging – Application to single virus-like particle entry into a cell. *Proc. Natl. Acad. Sci. USA* **99**, 16018–16023.
- 57** Zhang, H., Wu, L., Huang, F. (1999) Electrochemical microprocessing by scanning ion-conductance microscopy. *J. Vac. Sci. Technol. B* **17**, 269–272.
- 58** Lewis, A., Kheifetz, Y., Shambrodt, E., Radko, A., Khatchatryan, E., Sukenik, C. (1999) Fountain pen nanochemistry: Atomic force control of chrome etching. *Appl. Phys. Lett.* **75**, 2689–2691.
- 59** Müller, A.-D., Müller, F., Hietschold, M. (1998) Electrochemical pattern formation in a scanning near-field optical microscope. *Appl. Phys. A* **66**, S453–S456.
- 60** Müller, A.-D., Müller, F., Hietschold, M. (2000) Localized electrochemical deposition of metals using micro-pipettes. *Thin Solid Films* **366**, 32–36.
- 61** Hong, M.-H., Kim, K. H., Bae, J., Jhe, W. (2000) Scanning nanolithography using a material-filled nanopipette. *Appl. Phys. Lett.* **77**, 2604–2606.
- 62** Larson, B. J., Gillmor, S. D., Lagally, M. G. (2003) Controlled deposition of picoliter amounts of fluid using an ultrasonically driven micropipette. *Rev. Sci. Instrum.* **75**, 832–836.
- 63** Ying, L., Bruckbauer, A., Rothery, A. M., Korchev, Y. E., Klenerman, D. (2002) Programmable delivery of DNA through a nanopipet. *Anal. Chem.* **74**, 1380–1385.
- 64** Bruckbauer, A., Ying, L., Rothery, A. M., Zhou, D., Shevchuk, A. I., Abell, C., Korchev, Y. E., Klenerman, D. (2002) Writing with DNA and protein using a nanopipet for controlled delivery. *J. Am. Chem. Soc.* **124**, 8810–8811.
- 65** Bruckbauer, A., Zhou, D., Ying, L., Korchev, Y. E., Abell, C., Klenerman, D. (2003) Multicomponent submicron features of biomolecules created by voltage controlled deposition from a nanopipet. *J. Am. Chem. Soc.* **125**, 9834–9839.
- 66** Taha, H., Marks, R. S., Gheber, L. A., Rousso, I., Newman, J., Sukenik, C., Lewis, A. (2003) Protein printing with an atomic force sensing nanofountainpen. *Appl. Phys. Lett.* **83**, 1041–1043.
- 67** Rodolfa, K. T., Bruckbauer, A., Zhou, D., Korchev, Y. E., Klenerman, D. (2005) Two-component graded deposition of biomolecules with a double-barreled nanopipette. *Angew. Chem. Int. Ed.* **117**, 7014–7019.
- 68** Rodolfa, K. T., Bruckbauer, A., Zhou, D., Shevchuk, A. I., Korchev, Y. E., Klenerman, D. (2006) Nanoscale pipetting for controlled chemistry in small arrayed water droplets using a double-barrel pipet. *Nano Lett.* **6**, 252–257.
- 69** Ying, L., Bruckbauer, A., Zhou, D., Gorelik, J., Shevchuk, A., Lab, M., Korchev, Y., Klenerman, D. (2005) The scanned nanopipette: a new tool for high resolution bioimaging and controlled deposition of biomolecules. *Phys. Chem. Chem. Phys.* **7**, 2859–2866.
- 70** Seebach, J. (2001) *Einsatz elektrisch leitender Kultursubstrate zur Charakterisierung von Zell-Zell- und Zell-Substrat-Interaktionen*. Dissertation thesis, University of Münster, Münster.